

Lanthanide Triple Helical Complexes with a Chiral Bis(benzimidazole)pyridine Derivative

Gilles Muller,^[a,b] James P. Riehl,^[b] Kurt J. Schenk,^[c] Gérard Hopfgartner,^[d] Claude Piguet,^[e] and Jean-Claude G. Bünzli*^[a]

Keywords: Lanthanides / Tridentate ligands / Chirality / Luminescence / Stability constants

The ligand neopentyl 2,6-bis[(1-methylbenzimidazol-2-yl)]pyridine-4-carboxylate (**L**¹²) has been synthesised to test the effect of the chiral neopentyl ester group in the 4-position of the pyridine ring on (i) the helical wrapping, (ii) the diastereomeric induction and (iii) the thermodynamic and photophysical properties of the [Ln(**L**¹²)₃]³⁺ complexes. The crystal structure of ligand **L**¹² shows the expected *trans-trans* conformation of the tridentate binding unit. The ligand forms stable 1:3 complexes in anhydrous acetonitrile (logβ₃ in the range 17.3–19.0, logK₃ in the range 2.9–4.6). The triple helical structure in solution is responsible for the four times

larger specific rotary dispersion measured in the complexes. Circularly polarised luminescence of the Eu triple helical complex displays a weak effect, suggesting a small diastereomeric excess in solution. Ligand **L**¹² appears to favour a ³ππ*-to-Ln energy transfer process for Eu, but temperature-dependent nonradiative processes lead to a very small quantum yield. High-resolution luminescence spectra indicate that the Eu complex has a distorted D₃ local symmetry at the metal ion site.

(© Wiley-VCH Verlag GmbH, 69451 Weinheim, Germany, 2002)

Introduction

During the last two decades, lanthanide ions Ln^{III} have proved to be powerful luminescent and magnetic probes in biology and medicine.^[1–4] In the latter field, applications range from diagnosis (e.g. fluoroimmunoassays,^[5–7] luminescent specific imaging agents for tissues,^[8,9] contrast agents for magnetic resonance imaging^[10]) to therapeutic tools.^[11] In addition, these ions are also good catalysts for the selective hydrolysis of DNA and RNA.^[12,13]

These applications require the introduction of the Ln^{III} ions into functional molecular edifices able to preserve or better enhance the metal ion physicochemical properties.^[14] One strategy proposed to meet this goal is the formation of

induced cavities obtained by the self-assembly of carefully tailored multidentate ligands and podands.^[15] A judicious design of the ligands results in weak noncovalent interstrand interactions stabilizing the molecular edifices. We have shown that tridentate aromatic ligands **L**¹–**L**⁹, **L**¹¹ derived from bis(benzimidazole)pyridine (Scheme 1) lead to triple helical assemblies displaying sizeable ππ-stacking interactions, whose structural, photophysical and thermodynamic properties can be tuned by varying the substituents R¹, R² and R³.^[16–18] Substitution in the R² position of the benzimidazole rings essentially controls the stability and the final structure of the complexes, while substitution in the R¹ and R³ positions affects the electronic and photophysical properties.

So far, limited attention has been devoted to the inherent chirality of triple helical complexes, which often appear as racemic mixtures both in the solid state and in solution. However, Riehl et al. have shown that the [Ln(dpa)₃]³⁻ racemate equilibrium (H₂dpa = dipicolinic acid) can be perturbed by adding chiral sugars.^[19] Moreover, a small excess of one enantiomer can be induced in the excited state with the use of circular polarised excitation light.^[20] Chiral lanthanide complexes are of potential great interest because of their use as probes for the sensing of chirality in biological substrates.^[21,22] Since the high lability of the Ln^{III} ions favours easy racemisation of triple helical complexes, we are exploring the possibility of producing edifices in which the

^[a] Institute of Molecular and Biological Chemistry, Swiss Federal Institute of Technology
BCH 1402,
1015 Lausanne, Switzerland

E-mail: jean-claude.bunzli@epfl.ch

^[b] Department of Chemistry, University of Minnesota Duluth,
Minnesota 55812–2496, USA

^[c] Institute of Crystallography, BSP, University of Lausanne,
1015 Lausanne, Switzerland

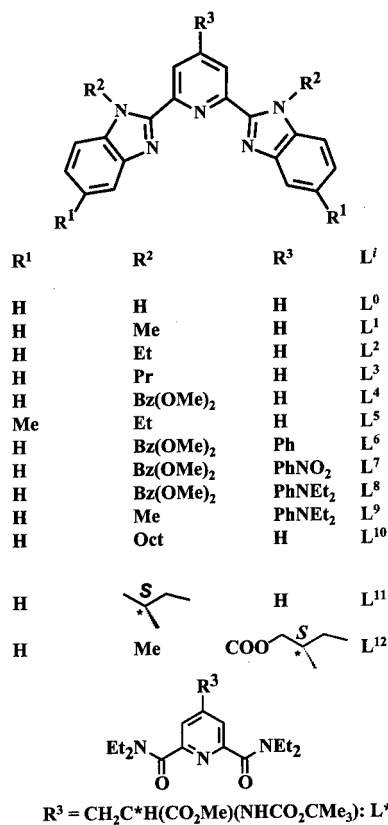
^[d] School of Pharmacy, University of Geneva,
Switzerland,

30 quai E. Ansermet, 1211 Geneva 4, Switzerland

^[e] Department of Inorganic, Analytical and Applied Chemistry,
University of Geneva,

30 quai E. Ansermet, 1211 Geneva 4, Switzerland

Supporting information for this article is available on the WWW under <http://www.ejic.com> or from the author.



Scheme 1

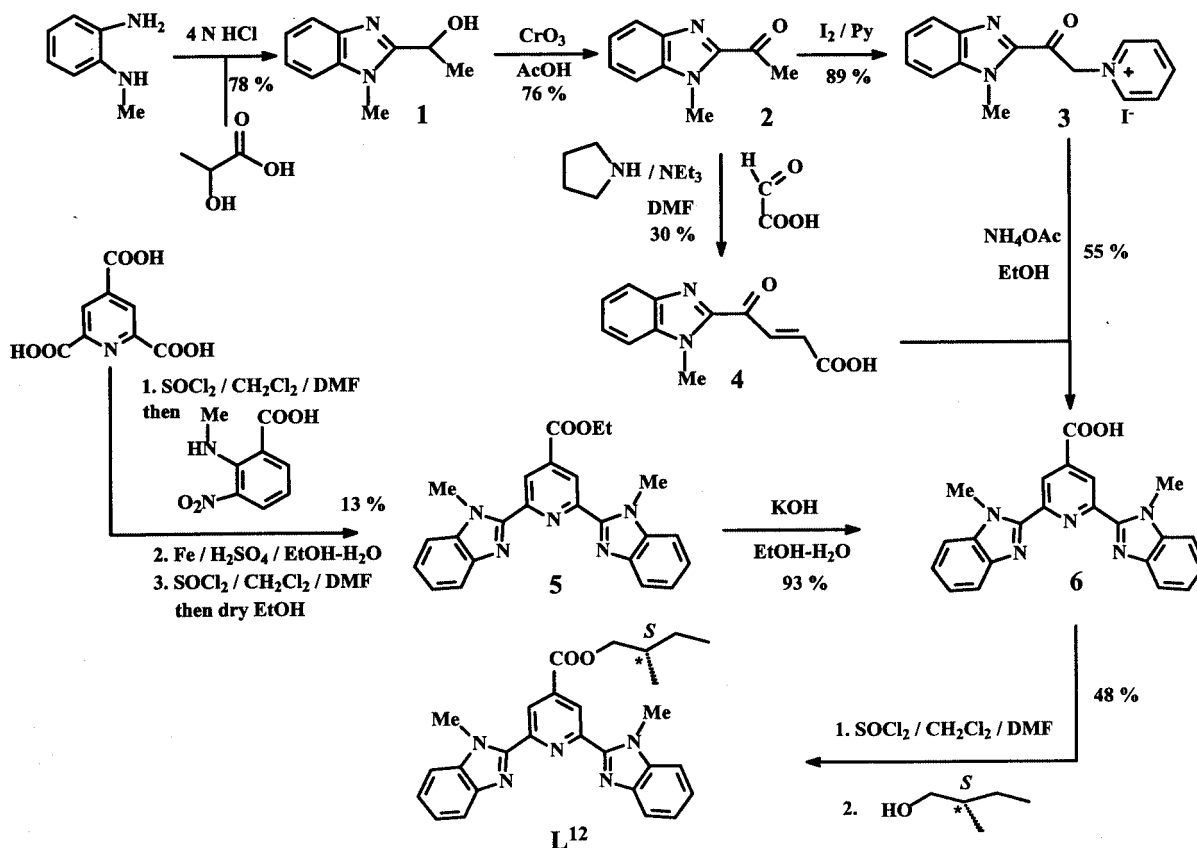
chirality is brought about by the ligands, a method which can only be used if the diastereoisomers have a large enough energy difference.

Working along these lines, we have introduced a chiral substituent onto the benzimidazole side arms of bis(benzimidazole)pyridine to yield **L¹¹**. Unfortunately, the bulky neopentyl group precludes the formation of stable triple helical complexes.^[18] On the other hand, introducing a bulky chiral substituent in the 4-position (**R³**) of a pyridine 2,6-dicarboxamide (**L^{*}**, Scheme 1) results in (i) helical wrapping of the three ligand strands around the Ln^{III} ion, (ii) thermodynamically stable 1:3 complexes (log*K*₃ in acetonitrile is in the range 5.1–5.3), and (iii) a small excess of one diastereoisomer.^[23] To further our understanding of the influence of helical wrapping on diastereomeric induction, we introduce here a chiral neopentyl ester group in the pyridine **R³** position of **L¹** (**L¹²**, Scheme 1), and investigate its influence on the thermodynamic, chiro-optical and luminescent properties of the resulting tris complexes with Ln^{III} ions.

Results and Discussion

Synthesis and Characterisation of the Ligand and its Complexes

Ligand **L¹²** was synthesised in a 48% yield from 2,6-bis[(1-methylbenzimidazol-2-yl)]pyridine-4-carboxylic acid (**6**) by esterification with (–),(*S*)-2-methyl-1-butanol (Scheme 2), while **6** was initially obtained by a four-step



Scheme 2

procedure involving a modified double Phillips coupling reaction to form the benzimidazole unit.^[24] Using an excess of *N*-ethyl-2-nitroaniline and 2,4,6-pyridinetricarboxylic acid favoured the formation of by-products such as the triamide, and significantly decreased the yield of the Phillips reaction. Consequently, we turned to a different strategy based on a procedure similar to that reported for the synthesis of **L**⁷ and **L**⁸,^[25] and made use of the Kröhnke reaction^[26] for the construction of the 4-substituted central pyridine ring. The required pyridinium salt **3** was prepared by an Ortoleva–King reaction^[27] from 2-acetyl-1-methylbenzimidazole (**2**), while 4-(1-methylbenzimidazol-2-yl)-4-oxo-2-butanoic acid (**4**) was obtained by a Knoevenagel condensation.^[26,28] Finally, **4** was synthesised by treating **2** with a mixture of glyoxylic acid monohydrate, triethylamine and pyrrolidine, which gave a better yield (30%) and resulted in an easier isolation process than the originally proposed method based on UV-irradiation.^[29]

The specific rotary dispersion of **L**¹² in degassed anhydrous acetonitrile, $[\alpha]_D^{25} = 8.1 \pm 0.4 \text{ deg dm}^2 \text{ mol}^{-1}$, confirms the chirality arising from the asymmetric carbon atom. At room temperature, the ¹H and ¹³C NMR spectra in CDCl₃ ($5 \times 10^{-3} \text{ M}$) display 13 and 17 signals, respectively, indicating a local pseudo twofold symmetry for the bis(benzimidazole)pyridine part of the molecule (Figure 1, Figure S1). These spectra coupled with $\{^1\text{H}-^1\text{H}\}$ COSY, DEPT-135, $\{^1\text{H}-^{13}\text{C}\}$ HSQC experiments and NOE effects observed between H⁴ and N–Me (NOE effects do not exist between H⁵ and N–Me), clearly suggest that **L**¹² has a *trans-trans* conformation, similar to that observed in **L**¹¹. This conformation also prevails in the solid state, as demonstrated by the X-ray crystal structure (Table 1, Figure 2). The unit cell contains two independent molecules A and B, the bond lengths and angles of which differ only slightly (Table S1). All aromatic groups are planar, but the benzimidazole units are not coplanar with the pyridine group, the interplanar angles being either very similar (16.6° and 10.9°) or largely different (36.3° and 14.2°) in molecules A and B, respectively (Table S2). These angles result in an optimal packing coefficient. Finally, no noteworthy hydrogen-bonding or π -stacking interactions exist in the structure, which seems to be an example of a pure van der Waals packing.

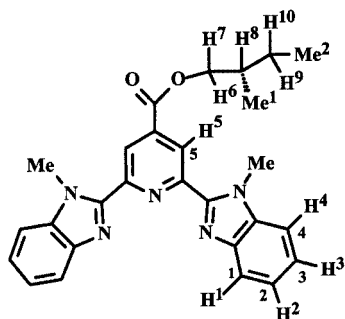


Figure 1. Numbering scheme for ligand **L**¹².

Table 1. Crystal data for **L**¹².

Formula	C ₂₇ H ₂₇ N ₅ O ₂
<i>M</i>	453.54
Crystal system	orthorhombic
Space group	<i>P</i> 2 ₁ 2 ₁ 2 ₁
<i>a</i> Å	7.302(5)
<i>b</i> Å	16.582(5)
<i>c</i> Å	39.001(5)
<i>V</i> Å ³	4722(4)
<i>Z</i>	8
<i>T</i> /K	170(1)
$\mu(\text{Mo}-K\alpha)/\text{mm}^{-1}$	0.083
Reflections measured	15587
Independent reflections	6273 ($R_{\text{int}} = 0.1013$)
Observed reflections [$F_0 \geq 4\sigma(F_0)$]	4529
Final <i>R</i> ₁ , <i>wR</i> ₂ [$I > 2\sigma(I)$]	0.0743, 0.1306

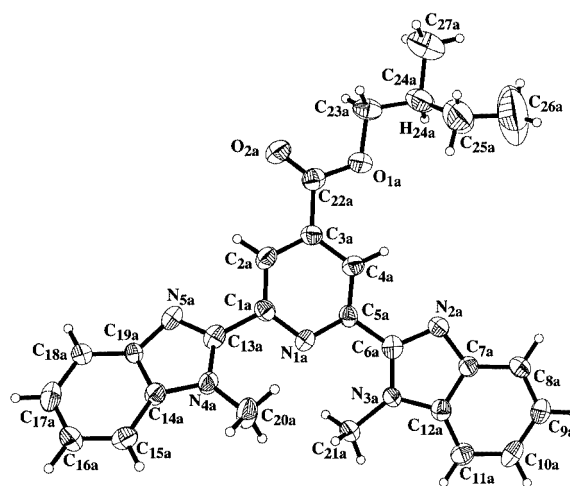


Figure 2. Molecular structure and atom numbering scheme for the two types of **L**¹² molecules found in the unit cell.

The 1:3 complexes were obtained in 70–80% yields, by adding a solution of **L**¹² in CH₂Cl₂ to solutions of lanthanide perchlorates in a mixture of MeCN and CH₂Cl₂. Evidence for complexation is the blue shift of the ν_{CO} and the two $\nu_{\text{C}=\text{C}}$ pyridine and benzimidazole vibrations by 4–6 cm⁻¹ and 2–6 cm⁻¹, respectively. All perchlorate ions are ionic; hence the complexes are most probably nine-coordinate (see below). Single crystals for X-ray structure determination could not be obtained.

Interactions between **L**¹² and the Ln^{III} Ions

The various species in solution were first identified by ESI-MS. Solutions of **L**¹² (10^{-4} M in anhydrous acetonitrile) were titrated with Ln(ClO₄)₃·*x*H₂O ($x = 0.2-0.6$) at 298 K, for ratios $R = [\text{L}^{12}]/[\text{Ln}^{\text{III}}]$, = 0–3. The spectra clearly show the successive formation of 1:*n* ($n = 1-4$) species, some of which had solvation molecules and/or were in the

Table 2. Relative intensities of the ESIMS peaks for solutions with $[\text{L}^{12}]/[\text{Ln}^{\text{III}}]_r = 3$ (MeCN, 298 K)

Species	La	Eu	Lu
$[\text{Ln}(\text{L}^{12})_3]^{3+}$	100	100	0.0
$[\text{Ln}(\text{L}^{12})_4]^{3+}$	16.7	17.8	0.0
$[\text{Ln}(\text{L}^{12})_2(\text{ClO}_4)]^{2+}$	7.5	9.2	0.0
$[\text{Ln}(\text{L}^{12})_3(\text{ClO}_4)]^{2+}$	12.5	0.0	0.0
$[\text{Ln}(\text{L}^{12})_3(\text{MeCN})_4]^{3+}$	0.0	0.0	100
$[\text{Ln}(\text{L}^{12})_2(\text{MeCN})]^{3+}$	0.0	0.0	75

form of perchlorate adducts (Table 2, Table S3). For La and Eu, the 1:3 complex ($R = 3$) is most abundant, while for Lu, this species coexists in solution with the 1:2 complex. In parallel, the proportion of the $[\text{Ln}(\text{L}^{12})_4]^{3+}$ species is relatively important for the larger ions (La, Eu), but this species is not seen for Lu. Such complexes have been observed for ligands derived from pyridine 2,6-dicarboxamide and were assigned to an outer-sphere association of a fourth ligand with a 1:3 complex.^[23,30] The ES-MS data clearly point to the presence of stable 1:3 complexes with La and Eu, while the formation of this species with Lu appears to be less favoured.

To confirm the speciation, the titration of L^{12} (10^{-3} M in CD_3CN) with La^{III} and Lu^{III} ions has been monitored by 400 MHz ^1H NMR spectroscopy. Chemical shifts are reported in Table 3, while Figure S2 (see Supporting Information) presents the aromatic part of the spectra obtained with Lu. Signals for the 1:1, 1:2, and 1:3 complexes could clearly be identified for both ions. When R reaches 3, the tris species is the major complex in solution for La (> 68%) and Lu (50%); the other species in solution is the 1:2 complex. This observation confirms that the bulky neopentyl ester group increases the steric constraint in the triple helical complexes with the smaller lanthanide ions. The stability constants extracted from ^1H NMR spectroscopic data and analysed with MINEQL⁺ [31] are reported in Table 4. The apparent ease with which the 1:3 complex forms contrasts with the situation observed with L^{11} , and indicates that the substitution in the R^3 position of the central pyridine is less detrimental to the formation of the helical complexes compared with substitution on the benzimidazole rings.^[18]

Table 3. ^1H NMR shifts observed (ppm) for L^{12} in CDCl_3 and for its 1:1, 1:2, and 1:3 complexes with Ln^{III} ions in CD_3CN (10^{-3} M, 298 K).

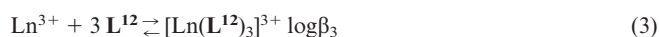
Species	H ¹	H ²	H ³	H ⁴	H ⁵	H ^{6,7}	H ⁸	H ^{9,10}	Me	Me ¹	Me ²
L^{12}	7.90	7.32–7.43		7.48	8.92	4.23, 4.32	1.95	1.29, 1.56	4.24	1.04	0.97
La 1:1	8.31	7.56–7.65		7.81	8.78	4.36, 4.41	1.96	1.39, 1.62	4.32	1.10	1.02
La 1:2	7.59	7.28	6.91	7.20	8.87	4.40, 4.46	2.03	1.44, 1.66	4.34	1.14	1.05
La 1:3	7.74	7.35	6.83	7.16	8.03	4.31, 4.35	1.92	1.37, 1.56	3.82	1.07	1.02
Lu 1:1	8.12	7.67	7.63	7.87	8.91	4.39, 4.44	2.04	1.46, 1.52	4.41	1.12	1.03
Lu 1:2	7.56	7.34	7.09	6.98	9.00	4.45, 4.52	2.06	1.45, 1.68	4.24	1.17	1.07
Lu 1:3	7.82	7.43	7.49	7.68	8.81	4.25, 4.30	1.94	1.35, 1.58	4.28	1.06	0.99

Table 4. Stability constants of $[\text{Ln}(\text{L}^{12})_n]^{3+}$ complexes ($n = 1-3$) as determined by NMR spectroscopy and UV/Vis spectrometry ($\mu = 0.1$ M Et_4NClO_4 , 298 K, $\pm 2\sigma$)

Ln	Log K_1		log K_2		log K_3	
	UV/Vis	NMR	UV/Vis	NMR	UV/Vis ^[a]	NMR
La	7.8 ± 0.4	8.0 ± 0.2	6.0 ± 0.5	6.0 ± 0.3	3.8 ± 0.6	3.8 ± 0.3
Eu	8.0 ± 0.3	^[b]	6.4 ± 0.4	^[b]	4.6 ± 0.5	^[b]
Lu	8.0 ± 0.3	7.9 ± 0.2	6.4 ± 0.4	6.5 ± 0.3	2.9 ± 0.4	3.1 ± 0.3

^[a] Values of log K_1 and log K_2 were fixed. ^[b] Not determined.

To quantify the $\text{Ln}^{\text{III}}-\text{L}^{12}$ interaction further, we have performed spectrophotometric titrations of L^{12} with $\text{Ln}(\text{Otf})_3$ ($\text{Ln} = \text{La, Eu, Lu}$; $\text{Otf} = \text{trifluoromethanesulfonate}$) at 298 K in MeCN, in the presence of 0.1 M Et_4NClO_4 , under anhydrous conditions ($[\text{H}_2\text{O}] < 30$ ppm). Factor analysis^[32] indicates the presence of three or four absorbing species and the data can be fitted to Equations (1)–(3), where solvation and anion coordination has been omitted.



A model including $[\text{Ln}(\text{L}^{12})_4]^{3+}$ does not improve the fit, in agreement with the postulated outer-sphere nature of this species detected in the gas phase. Electronic spectra of the three complexes are correlated, which renders the fitting process difficult and generates relatively large uncertainties in the $\log \beta_i$ values (Table 4). The stability constants are in a good agreement with those extracted from NMR spectroscopic data. The interactions between L^{12} and the Ln^{III} ions are stronger than those with L^{11} , as indicated by $\Delta \log K_3(\text{L}^{12}-\text{L}^{11}) = 2.6$ and 3.7 for La and Eu, respectively.^[18] According to previous studies with ligands derived from bis(benzimidazole)pyridine,^[17] the methyl substituents bound to the benzimidazole side arms in L^{12} favour the formation of a tight cavity around the lanthanide ions. This is not the case for the neopentyl groups in L^{11} . This observation also confirms the large influence of the alkyl N -substituents on the formation of the 1:3 complexes. However, the size-discriminating effect along the lanthanide series, and the stability of the $[\text{Ln}(\text{L}^i)]^{3+}$ complexes, are largely influenced by the substituents on the benzimidazole and

central pyridine groups; the latter acting on the electron density of the pyridyl N atom. The introduction of an electron-attracting neopentyl ester group in **L**¹² decreases the electronic density on the pyridyl N atom, which reduces the electrostatic interaction, as indicated by $\Delta \log K_3(\mathbf{L}^1 - \mathbf{L}^2) = 1.0 - 1.1$, but the size-discriminating effect is retained.^[17]

The specific rotary dispersion of solutions of the $[\text{Ln}(\mathbf{L}^{12})_3]^{3+}$ complexes (10^{-3} M in anhydrous acetonitrile) is 33.5 ± 0.5 (La) and 31.0 ± 0.3 deg dm² mol⁻¹ (Eu). This is about four times larger than those measured for the free ligand. We assign the greater rotary dispersion with respect to that generated by three free ligands to a structural contribution such as the formation of triple helical complexes in solution, as observed for **L***.^[23] As a comparison, relatively little or no ($4 - 5$ deg dm² mol⁻¹) structural contribution was observed for the 1:1 and 1:2 complexes with **L**¹¹.^[18] The circularly polarised luminescence (CPL) spectrum of a 5×10^{-3} M solution of $[\text{Eu}(\mathbf{L}^{12})_3]^{3+}$ is plotted in Figure 3 in the spectral range of the ⁵D₀ → ⁷F₁ transition,

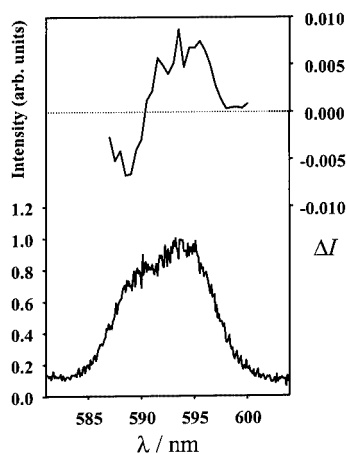


Figure 3. CPL spectrum of the ⁵D₀ → ⁷F₁ transition of $[\text{Eu}(\mathbf{L}^{12})_3]^{3+}$ (5×10^{-3} M in anhydrous MeCN at 295 K), on ligand excitation at 386 nm.

which is particularly well-suited for CPL measurements since it satisfies the magnetic-dipole selection rule, $\Delta J = 0, \pm 1$. The spectrum depends on the polarisation of the excitation light, indicating the presence of two species in solution.^[33] At the concentrations used, 93% of the Eu^{III} ion is in the form of the 1:3 complex, and 7% in the form of the 1:2 species, which is expected to generate a smaller chiral effect. The second species could also be a complex in which partial decomplexation of a ligand strand is induced by the interaction with one water molecule (see below). In conclusion, the CPL data are consistent with the presence of a small excess of one diastereoisomer in solution, on the short time scale of optical measurements, as previously observed for the corresponding complex with **L***.^[23]

Photophysical Properties

The electronic spectrum of **L**¹² in MeCN displays two intense bands centred around 33950 and 29590 cm⁻¹, with a shoulder at higher energy (Table 5, Figure 4). Irradiation in the UV region at room temperature yields one broad unresolved fluorescence band, centred around 22885 cm⁻¹ and originating from the ¹ππ* level (Figure 5). At 77 K, the fluorescence band is more structured and emission from the

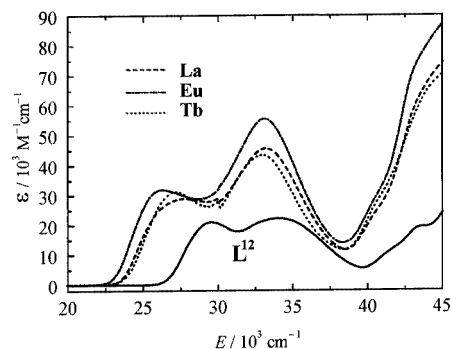


Figure 4. UV/Vis spectra of **L**¹² and its $[\text{Ln}(\mathbf{L}^{12})_3]^{3+}$ complexes (10^{-3} M in anhydrous MeCN at 293 K).

Table 5. Ligand-centred absorptions in acetonitrile and in the solid state (293 K), ligand-centred singlet- and triplet-state energies as determined from the emission spectra of the solids (77 K) and of the solutions (10^{-3} M in acetonitrile at 293 K) for the ligand **L**¹² and its triple helical complexes $[\text{Ln}(\mathbf{L}^{12})_3]^{3+}$.

Compnd	$E(x \rightarrow \pi^*)/\text{cm}^{-1}$ ^[a] Solution ^[b]	$E(^1\pi\pi^*)/\text{cm}^{-1}$		$E(^3\pi\pi^*)/\text{cm}^{-1}$ solid state ^[c]
		solid state	solution	
L ¹²	43480 (4.28) sh ^[d]	43480 sh		
	33950 (4.35)	33670		20920
	29590 (4.32)	27100	22885	17670
$[\text{La}(\mathbf{L}^{12})_3]^{3+}$	42980 (4.76) sh	45660 sh		
	33220 (4.66) 27630 (4.46)	34485		19750
		24940	21210	17990
$[\text{Eu}(\mathbf{L}^{12})_3]^{3+}$	43670 (4.89) sh	41490 sh		
	33115 (4.74) 26255 (4.50)	35715		
		24215	21100	[e]
$[\text{Tb}(\mathbf{L}^{12})_3]^{3+}$	43945 (4.81) sh	39215 sh		
	32980 (4.64) 27175 (4.49)	33670		
		24450	21645	21050

^[a] $x = n$ or π . ^[b] At the concentration used, 67–85% of the metal ion is in the form of the 1:3 complex and 15–33% in the form of the 1:2 complex; Log ϵ values are given in parentheses. ^[c] The 0-phonon transition is given in italics for frozen solutions in acetonitrile. ^[d] sh = shoulder. ^[e] not observed because of the **L**¹²-to-Ln energy transfer process.

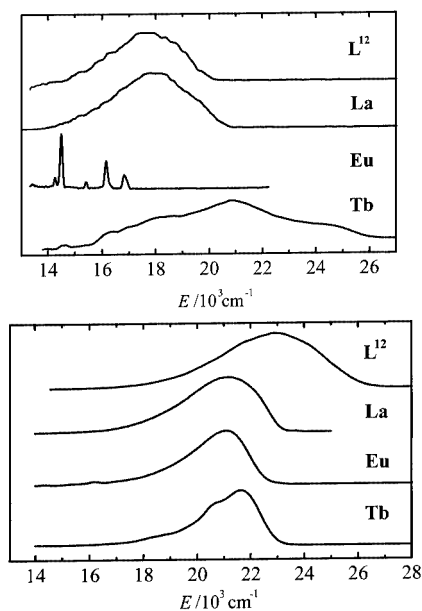


Figure 5. Top: Time-resolved emission spectra of **L**¹² and [Ln(**L**¹²)₃]³⁺ in the solid state at 77 K and recorded with time delays of 0.01 (Eu), 0.1 (Tb) and 10 ms (**L**¹², La). Bottom: Emission spectra of [Ln(**L**¹²)₃]³⁺ and **L**¹² (10⁻³ M in MeCN at 293 K).

³ππ* state appears with a maximum around 17670 cm⁻¹. The decay of the latter is a single exponential with a lifetime of 210 ± 3 ms, in the range of values previously reported for similar ligands (160–323 ms).^[16,34]

The higher energy component observed in the electronic (or reflectance) spectrum of **L**¹² at 33950 cm⁻¹ (33670 cm⁻¹) is only slightly modified on complexation with Ln^{III} ions, while the other band centred at 29590 cm⁻¹ (27100 cm⁻¹) undergoes an important red shift (Table 5, Figure 4). This observation reflects the electronic transformations associated with the *trans-trans*→*cis-cis* conformational change and the complexation of the lanthanide metal ions to the tridentate binding unit.^[16,25,34] On complexation of **L**¹² to La^{III}, the 0-phonon transitions of the singlet and triplet states are red-shifted by 1470 and 1170 cm⁻¹, respectively (frozen MeCN solution, 77 K, see Figure 5), and the ³ππ* lifetime decreases to 144 ± 1 ms. Emission from the ¹ππ* state of the ligand is still visible for the Eu and Tb complexes, suggesting an incomplete intersystem crossing. Emission from the ³ππ* state disappears for the Eu solution, with a concomitant observation of the metal-centred emission bands. This is not the case for the Tb solution for which little or no ligand-to-Tb energy transfer takes place because the energy of the ligand donor level (19750 cm⁻¹ in the La complex at 77 K) is located below the metal ⁵D₄ acceptor level (20350 cm⁻¹). Weak emission from the Tb^{III} ion can only be seen on direct excitation of the metal states (Figure S3, Supporting Information), and the short and temperature-dependent Tb(⁵D₄) lifetime (decreasing from 0.38 to 0.12 ms between 13 and 55 K) indicates that energy back transfer occurs in this complex.

In order to gain information on the chemical environment around the Eu^{III} ion, we have measured the high-res-

olution emission spectra of a solid state sample of [Eu(**L**¹²)₃](ClO₄)₃·2H₂O (**8**) at low temperature since this complex is only faintly luminescent at room temperature. The lifetime of the ⁵D₀ level, 0.85 ± 0.01 ms, is constant between 13 and 77 K. This is shorter than the lifetimes reported for [Eu(**L**¹)₃]³⁺ (1.85 ms in the range 4–77 K)^[35] and [Eu(**L**¹¹)₃]³⁺ (2.03 ms at 10 K),^[36] but similar to that found for [Eu(ClO₄)₂(H₂O)(**L**¹¹)₂]⁺ (0.65 ms at 10 K).^[36] Therefore, we cannot rule out the interaction of one water molecule in the first coordination sphere. The decrease in the Eu(⁵D₀) lifetime from 0.85 ms to 0.27 ms between 77 and 295 K indicates temperature-dependent quenching mechanisms, e.g. a ligand-to-metal charge transfer as demonstrated for [Eu(**L**¹)₃]³⁺,^[37,38] and as reported for other Eu^{III} complexes^[39] or other intermolecular interactions. In acetonitrile solution (10⁻³ M) at 295 K, the lifetime is longer, reaching 0.96 ± 0.01 ms; since in addition to the hydration of **8** the solvent contains about 2 mM H₂O, inner-sphere water interaction could occur. Using Horrocks equation, $q = 1.05 (k_{\text{H}_2\text{O}} - k_{\text{D}_2\text{O}})$ ^[40] and taking $k_{\text{D}_2\text{O}}$ equal to 0.51 ms⁻¹ (average of the values for the anhydrous tris species with **L**¹ and **L**¹¹),^[35,36] we find $q = 0.56$. This points to an equilibrium in solution between an anhydrous species and a monohydrate, as has been observed for triple helical complexes with terpyridine derivatives.^[41] Alternatively, it has been demonstrated that fast diffusing outer-sphere H₂O molecules can contribute 0.25 ms⁻¹ to the quenching of the Eu^{III} ion in complexes with cyclen derivatives.^[42] Applying a similar correction for **8** results in a reduction of q by approximately a factor of 2. Therefore, given the uncertainties linked to this type of correlation, it is difficult to determine from the lifetime data whether or not a water molecule interacts in the inner coordination sphere. On the other hand, it is clear that the introduction of an electron-attracting group in the R³ position weakens the Ln–N(py) bond, consistent with the relatively high energy of the ⁵D₀ ← ⁷F₀ transition (17258 cm⁻¹ at 295 K). Using the correlation proposed by Frey and Horrocks^[43] and the nephelauxetic parameter $\delta_{\text{N}(\text{het})} = -15.3 \text{ cm}^{-1}$ that we reported previously,^[44] we get $\delta_{\text{N}(\text{py})} = -8.1 \text{ cm}^{-1}$, a value much lower than those proposed (-12 to -17 cm⁻¹).^[43,45]

The emission spectra recorded at 13 K on excitation through the ligand band, or direct laser excitation of the ⁵D₀ ← ⁷F₀ transition, display fairly broad bands which are compatible with a distorted D₃ symmetry environment for the metal ion (Figure S4). The relative intensities of the ⁵D₀ → ⁷F_J transitions are 0.07, 1.00, 1.28, <0.01 and 4.11 for $J = 0, 1, 2, 3,$ and $4,$ respectively. The ⁵D₀ → ⁷F₁ transition displays two main components, one of them appearing as a doublet with a splitting of 17 cm⁻¹, while the ⁵D₀ → ⁷F₂ transition shows two doublets with a splitting of 13 and 14 cm⁻¹, respectively. Finally, the ⁵D₀ → ⁷F₄ transition displays four main components, three of them having a very weak intensity, again compatible with a distorted D₃ local symmetry.

To get a better insight into the various energy conversion processes occurring in the [Ln(**L**¹²)₃]³⁺ complexes, we have determined the quantum yields of both the ligand- and

metal-centred luminescence of 10^{-3} M solutions at 295 K, and the ratio between the integrated triplet and singlet state emissions, $I^{(T)}/I^{(S)}$ for the free ligand and its La^{III} complex at 77 K. The quantum yield of $[\text{La}(\text{L}^{12})_3]^{3+}$ ($Q^{\text{F}} = 5.5\%$) decreases by a factor of 9 with respect to that of the free ligand ($Q^{\text{F}} = 51\%$), and the ligand-centred phosphorescence increases, as indicated by $I^{(T)}/I^{(S)}$ which increases from 8×10^{-5} to 9.8×10^{-3} on complexation of L^{12} with La^{III} , that is by a factor of 122. The better intersystem crossing (isc) efficiency in the La^{III} complex may be explained by (i) the reduced energy gap between the $^1\pi\pi^*$ and $^3\pi\pi^*$ states: 2350 cm^{-1} , determined from the energy of the 0-phonon transitions, in contrast to 2650 cm^{-1} in the free ligand (Figure 6) and (ii) the spin-orbit mixing of the singlet and triplet states induced by the complexation with La^{III} .^[46] The quantum yield of the metal-centred luminescence of $[\text{Eu}(\text{L}^{12})_3]^{3+}$ obtained on ligand excitation remains very small, $Q_{\text{L}}^{\text{Eu}} = 5 \times 10^{-3} \%$, not only because the efficiency of the isc process stays small, but most probably because of photoinduced electron transfer processes, as already pointed out for the triple helical complex with L^1 .^[37,38]

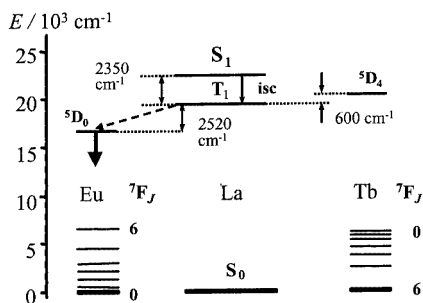


Figure 6. Schematic energy diagram for $[\text{Ln}(\text{L}^{12})_3]^{3+}$ complexes. Data for S_1 and T_1 are those of the La^{III} complex in the solid state at 77 K (0-phonon transitions).

Conclusion

The introduction of a chiral neopentyl ester group in the 4-position of the central pyridine ring of ligand L^1 to yield L^{12} leads to the formation of thermodynamically stable 1:3 complexes with lanthanide ions in acetonitrile, as shown by the $\log K_3$ values in the range 2.9–4.6. Chiro-optical data clearly suggest the helical wrapping of the ligand strands around the Ln^{III} ions. As a comparison, the bulky neopentyl groups grafted onto the benzimidazole side arms in L^{11} precluded helical wrapping, a fact confirmed by the specific rotary dispersion measurements.^[18] Although only a small excess of one diastereoisomer is induced in solution by the chiral ligand L^{12} , as was observed for complexes with L^* ,^[23] this work reveals that structural chirality may be induced in triple helical complexes by a suitable design of the ligand. The substitution also significantly modifies the photophysical properties of the tris complexes, compared with those with L^{11} .^[36] In particular, the ligand-to-metal energy transfer is amplified for Eu, but cancelled for Tb.

Therefore, this study demonstrates that, in addition to the electronic and photophysical properties which may be

modulated by varying the substituent in the R^3 position, a diastereomeric excess can be induced in solution if this substituent is chiral. The combination of these properties opens new perspectives for the design of lanthanide triple helical complexes acting as probes for chiral recognition.

Experimental Section

Solvents and Starting Materials: Acetonitrile, dichloromethane, chloroform, tetrahydrofuran, pyridine and triethylamine were purified in the usual way.^[47] Silica gel (Merck 60, 0.04–0.06 mm) was used for preparative column chromatography. Other products were purchased from Fluka AG (Buchs, Switzerland) or Merck and used without further purification. 2,4,6-pyridinetricarboxylic acid was prepared according to a literature procedure.^[48] Lanthanide perchlorates were obtained as described previously.^[49]

Caution: Dry perchlorates and their complexes with aromatic amines may easily explode and should be handled in small quantities and with extreme caution.^[50]

Spectroscopic and Analytical Measurements: Electronic spectra in the UV/Vis range were recorded at 293 K with a Perkin–Elmer Lambda 900 spectrometer and 1.0 and 0.1 cm quartz cells. Reflectance spectra were recorded on finely ground powders dispersed in MgO (5%), with MgO as the reference, on the same spectrometer equipped with a Labsphere PELA-1000 integration sphere. Specific rotary dispersion values were measured from 10^{-3} M solutions in degassed anhydrous acetonitrile at 298 K with the help of a JASCO DIP-370 polarimeter (sodium D line). IR spectra were obtained from KBr pellets with a Mattson α -Centauri FT-IR spectrometer. Pneumatically assisted electrospray (ESIMS) mass spectra were recorded from MeCN solutions on API III or API 3000 tandem mass spectrometers (PE Sciex) by infusion at $10 \mu\text{L min}^{-1}$. The spectra were recorded under low up-front declustering or collision-induced dissociation (CID) conditions, typically $\Delta V = 0–30$ V between the orifice and the first quadrupole of the spectrometer. ^1H , ^{13}C NMR spectra and 2-D experiments were recorded at 25 °C on Bruker AM-360 or Bruker AVANCE 400-DRX spectrometers. Chemical shifts are reported in parts per million with respect to TMS. Ligand excitation and emission spectra were recorded on a Perkin–Elmer LS-50B spectrometer equipped for low temperature (77 K) measurements. The experimental procedures for high resolution, laser-excited luminescence studies have been published previously.^[51] Emission spectra are corrected for the instrumental function. Quantum yields of the ligand-centred emission were measured relative to quinine sulfate in 0.05 M H_2SO_4 ($A_{347} = 0.05$, absolute quantum yield: 0.546).^[52] Quantum yields of the metal-centred emission were determined as described previously^[53] at excitation wavelengths at which (i) the Lambert–Beer law is obeyed and (ii) the absorption of the reference $[\text{Ln}(\text{terpy})_3]^{3+}$ closely matches that of the sample. CPL measurements were made on an instrument described previously, operating in a differential photon-counting mode.^[33] Elemental analyses were performed by Dr H. Eder (Microchemical Laboratory, University of Geneva).

Spectrophotometric Titrations: The electronic spectra in the UV/Vis range were recorded at 298 K from 10^{-4} M solutions in acetonitrile containing Et_4NClO_4 (0.1 M) as the inert electrolyte with a Perkin–Elmer Lambda 7 spectrometer connected to an external computer and in quartz cells of 0.100 cm path length. Solutions were prepared in a thermostatted vessel (Metrohm 6.1418.220) and the titrant solution was added with an automated burette from Me-

trohm (6.1569.150 or .210) fitted with an anti-diffusion device. In a typical experiment, 5–10 cm³ of L¹² were titrated with a solution of Ln^{III} triflate (10⁻⁴ M) in acetonitrile. After each addition of 0.20 cm³ and a delay of 2 min, the spectrum was measured and transferred to the computer. In some instances, reverse titrations, i.e. with L¹² as the titrating species, were also performed to confirm the values of the stability constants. All the experiments were conducted in a dry box and the water content of the solutions, measured at the end of the titration by the Karl Fischer method, was always <30 ppm. Factor analysis and stability constant determinations were carried out with the program SPECFIT, version 2.10.^[54]

Crystal Structure of L¹²: The pale yellowish, lathlike crystals were directly transferred from the mother liquor into a drop of Hostinert 216 oil kept at 210 K. A specimen was selected and placed in a glass capillary. The data collection, at 170 K, took place on a Stoe IPDS system equipped with Mo-K_α radiation (Table 1). The image plate – crystal distance was set to 80 mm, and a ϕ interval of 1° was chosen. Two hundred images were then exposed for 20 min each. Inspection of the reciprocal space revealed that about three quarters of the diffraction spots could be accounted for by the cell given in Table 1. The integration was based on an effective mosaic spread of 0.012 and a profile between 11 and 21 pixels. A peak overlap of 2 pixels was tolerated in order to retain the maximum number of reflections. Nevertheless, over 2700 reflections were eliminated because of severe peak overlap. The intensities were corrected for Lorentz and polarisation effects. No absorption correction could be applied since the crystal was all but invisible in the frozen oil, but the absorption coefficient appeared to be small. The decay during the measurement was negligible. The structure was solved in the space group *P*₂₁₂₁ with the help of SIR 97.^[55] The oxygen and nitrogen atoms were refined anisotropically and the carbon and hydrogen atoms isotropically; the latter were allowed to ride on their associated carbon atoms. The refinement seems to favour the *S* configuration for the chirality centre C24 for both molecules, as expected from the synthesis and the observed rotary dispersion, but the value of Flack's parameter (2 ± 2) is not conclusive.^[56] CCDC-186842 contains the supplementary crystallographic data for this paper, which can be obtained free of charge at www.ccdc.cam.ac.uk/conts/retrieving.html [or from the Cambridge Crystallographic Data Centre, 12 Union Road, Cambridge CB2 1EZ, UK; fax: (internat) +44-1223/336-033; E-mail: deposit@ccdc.cam.ac.uk].

Preparation of the Ligand. (±)-2-(1-Hydroxyethyl)-1-methylbenzimidazole (1): A mixture of *N*-Methyl-1,2-phenylenediamine (0.93 cm³, 8.18 mmol) and (±)-2-hydroxypropionic acid (0.91 cm³, 12.21 mmol) was refluxed for 45 min in 4 N hydrochloric acid (10 cm³). After cooling, the mixture was neutralised to pH = 7.1 with NH₄OH (25%). The resulting brown crude solid was filtered, washed with water and recrystallised from hot water to give 1.13 g of **1** (6.41 mmol, 78%). M.p. 106–108 °C. ¹H NMR (360 MHz, CD₃OD): δ = 1.73 (d, ³*J* = 7.0 Hz, 3 H), 3.94 (s, 3 H), 4.93 (s, 1 H), 5.20 (q, ³*J* = 7.0 Hz, 1 H), 7.25–7.34 (m, 2 H), 7.50 (m, 1 H), 7.66 (m, 1 H) ppm. ¹³C NMR (360 MHz, CD₃OD): δ = 21.65, 30.67, 64.15, 110.79, 119.59, 123.33, 124.06, 137.37, 142.35, 157.45 ppm. IR (KBr): $\tilde{\nu}$ = 1105 (ν_{C-OH}) cm⁻¹. ESI-MS (MeOH): *m/z* = 177.2 [L + H]⁺.

2-Acetyl-1-methylbenzimidazole (2): A solution of chromium trioxide (494 mg, 4.94 mmol) in water (3 cm³) was added dropwise to a solution of **1** (1.13 g, 6.41 mmol) in glacial acetic acid (5 cm³) at 90 °C. The reaction mixture was heated at 100 °C for 10 min and poured into water (60 cm³). The resulting precipitate was extracted with dichloromethane (3 × 30 cm³), and the combined extracts

dried (Na₂SO₄) and the solvents evaporated. The resulting crude solid was recrystallised from methanol to give 849 mg of **2** (4.87 mmol, 76%) as white crystals. M.p. 72–74 °C. ¹H NMR (360 MHz, CDCl₃): δ = 2.83 (s, 3 H), 4.11 (s, 3 H), 7.33–7.37 (m, 1 H), 7.41 (m, 2 H), 7.87 (m, 1 H) ppm. ¹³C NMR (360 MHz, CDCl₃): δ = 28.18, 32.38, 110.64, 122.02, 123.82, 126.06, 137.07, 141.71, 146.28, 193.46 ppm. IR (KBr): $\tilde{\nu}$ = 1684 (ν_{CO}) cm⁻¹. ESI-MS (MeOH): *m/z* = 175.1 [L + H]⁺.

1-[(Methylbenzimidazol-2-yl)carbonyl]methyl-1-pyridinium Iodide (3): **2** (211 mg, 1.21 mmol) and I₂ (307 mg, 1.21 mmol) were dissolved in dry distilled pyridine (4 cm³) under an inert atmosphere. After 20 min at room temp., the mixture was heated at 100 °C for 15 h, then cooled to room temperature. The resulting brown precipitate was filtered, washed once with pyridine/diethyl ether (1:1, 5 cm³) and twice with diethyl ether (10 cm³). The dried crude product was recrystallised from ethanol with charcoal to give 410 mg of **3** (1.08 mmol, 89%) as dark yellow needles. M.p. 205–207 °C. ¹H NMR (360 MHz, [D₆]DMSO): δ = 4.11 (s, 3 H), 6.54 (s, 2 H), 7.46 (m, 1 H), 7.56 (m, 1 H), 7.84 (m, 1 H), 7.94 (m, 1 H), 8.30 (m, 2 H), 8.76 (m, 1 H), 9.03 (m, 2 H) ppm. ¹³C NMR (360 MHz, [D₆]DMSO): δ = 31.96, 66.56, 111.86, 121.22, 124.22, 126.47, 127.74, 136.65, 141.07, 143.47, 145.56, 146.46, 184.43 ppm. IR (KBr): $\tilde{\nu}$ = 1705 (ν_{CO}) cm⁻¹. FAB-MS (MeOH): *m/z* = 252.1 [L – I]⁺.

4-(1-Methylbenzimidazol-2-yl)-4-oxobut-2-enoic Acid (4): Glyoxylic acid monohydrate (1 g, 10.86 mmol), triethylamine (1.52 cm³, 10.86 mmol) and pyrrolidine (0.33 cm³, 3.8 mmol) were sequentially added to a solution of **2** (631 mg, 3.62 mmol) in DMF (10 cm³). The mixture was stirred at room temp. for 48 h and 1% hydrochloric acid was then added until pH = 1. The solution was extracted with diethyl ether (3 × 20 cm³) and the combined organic layers were dried (Na₂SO₄) and the solvents evaporated. The resulting crude solid was redissolved with 10% NaHCO₃ (5 cm³) to pH = 8 and washed with dichloromethane (2 × 10 cm³). The aqueous phase was acidified to pH = 1 by addition of 10% hydrochloric acid and extracted with diethyl ether (3 × 10 cm³). The combined organic layers were washed with water (2 × 30 cm³), dried (Na₂SO₄) and the solvents evaporated. The resulting crude solid was recrystallised by slow diffusion of hexane into an ethyl acetate solution to give 251 mg of **4** (1.09 mmol, 30%) as brownish-red needles. M.p. 194–196 °C. ¹H NMR (360 MHz, [D₆]DMSO): δ = 4.15 (s, 3 H), 6.83 (d, ³*J* = 15.9 Hz, 1 H), 7.39 (m, 1 H), 7.50 (m, 1 H), 7.75 (m, 1 H), 7.88 (m, 1 H), 8.28 (d, ³*J* = 15.9 Hz, 1 H) ppm. ¹³C NMR (360 MHz, [D₆]DMSO): δ = 32.18, 111.64, 121.45, 123.85, 126.32, 132.46, 136.65, 137.03, 141.22, 146.17, 166.24, 181.66 ppm. IR (KBr): $\tilde{\nu}$ = 1707, 1670 (ν_{CO}) cm⁻¹. ESI-MS (MeOH): *m/z* = 231.2 [L + H]⁺.

Ethyl 2,6-Bis[(1-methylbenzimidazol-2-yl)pyridine-4-carboxylate (5): A mixture of 2,4,6-pyridinetricarboxylic acid (1 g, 4.7 mmol), freshly distilled thionyl chloride (15 cm³, 207 mmol) and DMF (0.12 cm³) was refluxed for 90 min in dry dichloromethane (40 cm³), evaporated and dried under vacuum for 60 min. The resulting solid was dissolved in dry dichloromethane (45 cm³), and a mixture of 2-nitro-*N*-ethylaniline (1.08 g, 7.1 mmol) and triethylamine (6.6 cm³, 47 mmol) in dry dichloromethane (30 cm³) was added dropwise under inert atmosphere. The solution was stirred for 2 h at room temperature, refluxed for 6 h and the solvents evaporated. The brown residue was partitioned between dichloromethane (3 × 100 cm³) and half-saturated aqueous NH₄Cl solution (100 cm³). The combined organic phases were dried (Na₂SO₄) and the solvents evaporated. The crude product was dissolved in a mixture of ethanol/water (250:55 cm³), and freshly activated iron powder (8 g,

143 mmol) and 25% hydrochloric acid (45.7 cm³, 352 mmol) were added. The solution was refluxed for 8 h under inert atmosphere. The excess of iron was filtered off, and the ethanol was distilled off under vacuum. Water was then added to bring the total volume to 100 cm³. The resulting solution was poured into dichloromethane (150 cm³). Na₂H₂edta·2H₂O (84 g, 236 mmol) in 150 cm³ water was then added, and the resulting mixture was neutralised to pH = 7 with 5 M aqueous potassium hydroxide; 30% H₂O₂ (1 cm³) was added and the pH adjusted to 8.3. After vigorous stirring for 30 min, the organic layer was separated and the aqueous phase extracted with dichloromethane (3 × 150 cm³). The combined organic phases were dried (Na₂SO₄) and the solvents evaporated. The resulting crude solid was dissolved in dry dichloromethane (40 cm³), then freshly distilled thionyl chloride (15 cm³, 207 mmol) and DMF (0.12 cm³) were added. The mixture was refluxed for 90 min, evaporated and dried under vacuum for 60 min. The crude product was cooled to 0 °C, then dry ethanol (20 cm³) was added dropwise. The resulting solution was allowed to stand at room temperature, stirred for 60 min, evaporated and dried under vacuum for 60 min. The residue was partitioned between dichloromethane (3 × 40 cm³) and half-saturated aqueous NH₄Cl solution (40 cm³). The combined organic phases were dried (Na₂SO₄) and the solvents evaporated. The resulting brownish-red crude solid was purified by column chromatography (silica gel, CH₂Cl₂/MeOH, 100:0 → 99:1) to give 251 mg of **5** (0.61 mmol, 13%). ¹H NMR (400 MHz, CDCl₃): δ = 1.46 (t, ³J = 7.0 Hz, 3 H), 4.25 (s, 6 H), 4.49 (q, ³J = 7.0 Hz, 2 H), 7.39 (m, 4 H), 7.48 (m, 2 H), 7.91 (m, 2 H), 8.95 (s, 2 H) ppm. ¹³C NMR (400 MHz, CDCl₃): δ = 14.97, 33.24, 62.89, 110.69, 121.05, 123.78, 124.66, 125.26, 137.91, 141.03, 143.36, 150.32, 151.33, 164.85 ppm. IR (KBr): $\tilde{\nu}$ = 1712 (ν_{CO}), 1597, 1562 (ν_{C=C}) cm⁻¹. ESI-MS (MeCN): *m/z* = 412.2 [L + H]⁺.

2,6-Bis[(1-methylbenzimidazol-2-yl)]pyridine-4-carboxylic Acid (**6**).

Procedure A: **3** (410 mg, 1.08 mmol), **4** (226 mg, 0.98 mmol) and ammonium acetate (3 g, 38.92 mmol) were dissolved in ethanol (25 cm³). The mixture was refluxed for 24 h under an inert atmosphere, and then slowly cooled to room temperature. The resulting white crystals were separated by filtration and recrystallised from hot methanol to give 230 mg of **6** (0.60 mmol, 55%). **Procedure B:** A solution of **5** (251 mg, 0.61 mmol) in a mixture of ethanol/water, 1:4 (5:20 cm³) containing potassium hydroxide (17 g, 303 mmol) was refluxed for 24 h. Ethanol was distilled off and the aqueous phase acidified to pH = 3 with 25% hydrochloric acid. The resulting precipitate was filtered off and washed with water to give 218 mg of **6** (0.57 mmol, 93%) as a white powder. M.p. >260 °C. ¹H NMR (360 MHz, [D₆]DMSO): δ = 4.37 (s, 6 H), 7.38–7.47 (m, 4 H), 7.78 (m, 2 H), 7.87 (m, 2 H), 8.81 (s, 2 H) ppm. ¹³C NMR (360 MHz, [D₆]DMSO): δ = 36.51, 114.78, 123.45, 126.27, 127.10, 128.81, 141.06, 146.18, 146.70, 153.00, 154.41, 166.54 ppm. IR (KBr): $\tilde{\nu}$ = 1716 (ν_{CO}), 1617, 1560 (ν_{C=C}) cm⁻¹. ESI-MS (MeCN): *m/z* = 384.2 [L + H]⁺, 767.4 [2L + H]⁺.

Neopentyl 2,6-Bis[(1-methylbenzimidazol-2-yl)]pyridine-4-carboxylate (L¹²): A mixture of **6** (430 mg, 1.12 mmol), freshly distilled thionyl chloride (3.62 cm³, 50 mmol) and DMF (0.03 cm³) was refluxed for 90 min in dry dichloromethane (10 cm³), evaporated and dried under vacuum for 60 min. A solution of (–)-(S)-2-methyl-1-butanol (1.2 cm³, 11.2 mmol) dried on molecular sieves was added to the resulting crude solid. After stirring for 30 min at room temp., the resulting violet solution was evaporated and the residue was redissolved in CHCl₃ (10 cm³). The organic phase was washed with water (3 × 20 cm³), then with half-saturated aqueous NH₄Cl (20 cm³), dried (Na₂SO₄) and the mixture evaporated to dryness. The resulting crude solid was purified by column chroma-

tography (silica gel, CH₂Cl₂/MeOH, 100:0 → 99:1) and recrystallised by slow diffusion of hexane into a dichloromethane solution to give 245 mg of L¹² (0.54 mmol, 48%) as white crystals. M.p. 186–188 °C. ¹H NMR (360 MHz, CDCl₃): δ = 0.97 (t, ³J = 7.3 Hz, 3 H), 1.04 (d, ³J = 6.8 Hz, 3 H), 1.29 (m, ³J = 7.3 Hz, 1 H, ²J = 13.6 Hz), 1.56 (m, ³J = 7.3 Hz, 1 H, ²J = 13.6 Hz), 1.95 (1 H, pseudo-oct., ³J = 6.3–7.3 Hz), 4.23 (dd, 1 H, ³J = 6.3 Hz), 4.24 (s, 6 H), 4.32 (dd, 1 H, ³J = 6.3 Hz), 7.35–7.43 (m, 4 H), 7.48 (m, 2 H), 7.90 (m, 2 H), 8.92 (s, 2 H) ppm. ¹³C NMR (360 MHz, CDCl₃): δ = 11.35, 16.59, 26.20, 32.68, 34.34, 70.96, 110.15, 120.60, 123.20, 124.10, 124.68, 137.35, 140.51, 142.79, 149.78, 150.79, 164.44 ppm. IR (KBr): $\tilde{\nu}$ = 1730 (ν_{CO}), 1587, 1564 (ν_{C=C}) cm⁻¹. ESI-MS (MeCN): *m/z* = 454.2 [L + H]⁺. C₂₇H₂₇N₅O₂·0.11CH₂Cl₂: calcd. C 70.3, H 5.9, N 15.1; found C 70.3, H 6.0, N 15.1.

Preparation of the Complexes: The 1:3 complexes [Ln(L¹²)₃](ClO₄)₃·xH₂O (La, x = 2, (7); Eu, x = 2, (8); Tb, x = 3, (9)) were prepared by mixing L¹² with stoichiometric amounts of Ln(ClO₄)₃·nH₂O (Ln = La, Eu, Tb and n = 0.2–0.6) in dichloromethane/acetonitrile. The complexes may be crystallised in 70–80% yields by slow diffusion of *tert*-butyl methyl ether into an acetonitrile solution. [C₈₁H₈₁N₁₅O₁₈Cl₃La·2H₂O]: found C 53.2, H 4.6, N 11.6, calcd. C 53.1, H 4.7, N 11.5; C₈₁H₈₁N₁₅O₁₈Cl₃Eu·2H₂O: found C 52.5, H 4.7, N 11.4, calcd. C 52.7, H 4.6, N 11.4; C₈₁H₈₁N₁₅O₁₈Cl₃Tb·3H₂O: found C 51.9, H 4.5, N 11.1; calcd. C 52.0, H 4.7, N 11.2]. IR (KBr): $\tilde{\nu}$ = 1736 (La), 1735 (Eu), 1734 (Tb), (ν_{CO}); 1593, 1568 (La), 1591, 1570 (Eu), 1589, 1570 (Tb), (ν_{C=C}) and 1092, 625 (ionic ClO₄⁻) cm⁻¹.

Acknowledgments

This work is supported through grants from the Swiss National Science Foundation. We thank Prof. Pierre Vogel for the use of his polarimeter, Dr. Anne-Sophie Chauvin for her help in the ligand synthesis and the Fondation Herbette (Lausanne) for the gift of spectroscopic equipment.

- [1] J.-C. G. Bünzli in *Lanthanide Probes in Life, Chemical and Earth Sciences. Theory and Practice*, (Eds.: J.-C. G. Bünzli, G. R. Choppin), Elsevier Science Publ. B. V., Amsterdam, **1989**, Ch. 7, 219–293.
- [2] C. H. Evans, *Biochemistry of the Lanthanides*, Plenum Press, New York, **1990**.
- [3] D. Parker, *Coord. Chem. Rev.* **2000**, *205*, 109–130.
- [4] J.-C. G. Bünzli, C. Piguet in *Encyclopedia of Materials: Science and Technology* (Eds.: K. H. J. Buschow, R. W. Cahn, M. C. Flemings, B. Ilshner, E. J. Kramer, S. Mahajan), Elsevier Science Ltd, Oxford, **2001**, *10*, Ch. 1.10.4, 4465–4476.
- [5] G. Mathis in *Rare Earths*, (Eds.: R. Saez Puche, P. Caro), Editorial Complutense, Madrid, **1998**, 285–297.
- [6] I. Hemmilä, T. Ståhlberg, P. Mottram, *Bioanalytical Applications of Labelling Technologies*, Wallac Oy, Turku, **1995**.
- [7] V. W. W. Yam, K. K. W. Lo, *Coord. Chem. Rev.* **1999**, *184*, 157–240.
- [8] D. J. Bornhop, D. S. Hubbard, M. P. Houlne, C. Adair, G. E. Kiefer, B. C. Pence, D. L. Morgan, *Anal. Chem.* **1999**, *71*, 2607–2615.
- [9] G. E. Kiefer, L. Jackson, D. J. Bornhop, **1999**, US patent 5,928,627.
- [10] A. E. Merbach, E. Toth, *The chemistry of contrast agents in medical magnetic resonance imaging*, Wiley, London, **2001**.
- [11] Z. J. Guo, P. J. Sadler, *Angew. Chem. Intl. Ed. Engl.* **1999**, *38*, 1513–1531.
- [12] M. Komiyama, N. Takeda, H. Shigekawa, *Chem. Commun.* **1999**, 1443–1451.

- [13] G. Pratviel, J. Bernardou, B. Meunier, *Adv. Inorg. Chem.* **1998**, *45*, 251–312.
- [14] J.-C. G. Bünzli in *Rare Earths*, (Eds.: R. Saez Puche, P. Caro), Editorial Complutense, Madrid, **1998**, 223–259.
- [15] C. Piguet, J.-C. G. Bünzli, *Chem. Soc. Rev.* **1999**, *28*, 347–358.
- [16] C. Piguet, J.-C. G. Bünzli, G. Bernardinelli, C. G. Bochet, P. Froidevaux, *J. Chem. Soc., Dalton Trans.* **1995**, 83–97.
- [17] S. Petoud, J.-C. G. Bünzli, F. Renaud, C. Piguet, K. J. Schenk, G. Hopfgartner, *Inorg. Chem.* **1997**, *36*, 5750–5760.
- [18] G. Muller, J.-C. G. Bünzli, K. J. Schenk, C. Piguet, G. Hopfgartner, *Inorg. Chem.* **2001**, *40*, 2642–2651.
- [19] E. Huskowska, J. P. Riehl, *Inorg. Chem.* **1995**, *34*, 5615–5621.
- [20] S. C. J. Meskers, H. P. J. M. Dekkers, *J. Phys. Chem. A* **2001**, *105*, 4589–4599.
- [21] H. Tsukube, S. Shinoda, *Chem. Rev.* **2002**, *102*, 2389–2404.
- [22] L. J. Govenlock, C. E. Mathieu, C. L. Maupin, D. Parker, J. P. Riehl, G. Siligardi, J. A. G. Williams, *Chem. Commun.* **1999**, 1699–1700.
- [23] G. Muller, B. Schmidt, J. Jiricek, G. Hopfgartner, J. P. Riehl, J.-C. G. Bünzli, C. Piguet, *J. Chem. Soc., Dalton Trans.* **2001**, 2655–2662.
- [24] C. Piguet, B. Bocquet, G. Hopfgartner, *Helv. Chim. Acta* **1994**, *77*, 931–942.
- [25] C. G. Bochet, C. Piguet, A. F. Williams, *Helv. Chim. Acta* **1993**, *76*, 372–384.
- [26] F. Kröhnke, *Synthesis* **1976**, 1–24.
- [27] F. Kröhnke, *Angew. Chem. Intl. Ed. Engl.* **1963**, *2*, 225–228.
- [28] M. I. Ali, A. M. Abd-Elfattah, H. A. Hammouda, *Z. Naturforsch., Teil B* **1976**, *31*, 254–256.
- [29] M. J. Melo, F. Pina, A. L. Macanita, E. C. Melo, C. Herrmann, R. Förster, H. Koch, H. Wamhoff, *Z. Naturforsch., Teil B* **1992**, *47*, 1431–1437.
- [30] F. Renaud, C. Piguet, G. Bernardinelli, J.-C. G. Bünzli, G. Hopfgartner, *Chem. Eur. J.* **1997**, *3*, 1660–1667.
- [31] W. Schecher, MINEQL⁺ version 2.1, MD Environmental Research Software, Edgewater, NY, **1991**.
- [32] E. R. Malinowski, D. G. Howery, *Factor Analysis in Chemistry*, John Wiley, New York, Chichester, Brisbane, Toronto, **1980**.
- [33] J. P. Riehl, F. S. Richardson, *Chem. Rev.* **1986**, *86*, 1–18.
- [34] C. Piguet, A. F. Williams, G. Bernardinelli, E. Moret, J.-C. G. Bünzli, *Helv. Chim. Acta* **1992**, *75*, 1697–1717.
- [35] C. Piguet, A. F. Williams, G. Bernardinelli, J.-C. G. Bünzli, *Inorg. Chem.* **1993**, *32*, 4139–4149.
- [36] G. Muller, PhD. Dissertation, University of Lausanne, **2000**.
- [37] S. Petoud, J.-C. G. Bünzli, T. Glanzman, C. Piguet, Q. Xiang, R. P. Thummel, *J. Lumin.* **1999**, *82*, 69–79.
- [38] F. R. Gonçalves e Silva, R. L. Longo, O. L. Malta, C. Piguet, J.-C. G. Bünzli, *Phys. Chem. Chem. Phys.* **2000**, *2*, 5400–5403.
- [39] J. Bartis, M. Dankova, J. J. Lessmann, Q. H. Luo, W. deW. Horrocks, Jr., L. C. Francesconi, *Inorg. Chem.* **1999**, *38*, 1042–1053.
- [40] W. deW. Horrocks, Jr., D. R. Sudnick, *Acc. Chem. Res.* **1981**, *14*, 384–384.
- [41] C. Mallet, R. P. Thummel, C. Hery, *Inorg. Chim. Acta* **1993**, *210*, 223–231.
- [42] A. Beeby, I. M. Clarkson, R. S. Dickens, S. Faulkner, D. Parker, L. Royle, A. S. de Sousa, J. A. G. Williams, M. Woods, *J. Chem. Soc., Perkin Trans. 2* **1999**, 493–503.
- [43] S. T. Frey, W. deW. Horrocks, Jr., *Inorg. Chim. Acta* **1995**, *229*, 383–390.
- [44] S. Petoud, J.-C. G. Bünzli, K. J. Schenk, C. Piguet, *Inorg. Chem.* **1997**, *36*, 1345–1353.
- [45] M. Latva, J. Kankare, *J. Coord. Chem.* **1998**, *43*, 121–142.
- [46] S. Tobita, M. Arakawa, I. Tanaka, *J. Phys. Chem.* **1985**, *89*, 5649–5654.
- [47] D. D. Perrin, W. L. F. Armarego, *Purification of Laboratory Chemicals*, Pergamon Press, Oxford, **1988**.
- [48] L. Syper, K. Kloc, J. Mlochowski, *Tetrahedron* **1980**, *36*, 123–129.
- [49] J.-C. G. Bünzli, J.-R. Yersin, C. Mabillard, *Inorg. Chem.* **1982**, *21*, 1471–1476.
- [50] W. C. Wolsey, *J. Chem. Educ.* **1973**, *50*, A335–A337.
- [51] N. Martin, J.-C. G. Bünzli, V. McKee, C. Piguet, G. Hopfgartner, *Inorg. Chem.* **1998**, *37*, 577–589.
- [52] S. R. Meech, D. C. Phillips, *J. Photochem.* **1983**, *23*, 193–217.
- [53] H.-R. Mürner, E. Chassat, R. P. Thummel, J.-C. G. Bünzli, *J. Chem. Soc., Dalton Trans.* **2000**, 2809–2816.
- [54] H. Gampp, M. Maeder, C. J. Meyer, A. D. Zuberbühler, *Talanta* **1985**, *23*, 1133–1139.
- [55] A. Altomare, M. C. Burla, M. Camalli, G. L. Casciarano, C. Giacovazzo, A. Guagliardi, G. G. Moliterni, G. Polidori, R. Spagna, *J. Appl. Cryst.* **1999**, *32*, 115–119.
- [56] H. D. Flack, *Acta Crystallogr., Sect. A* **1983**, *39*, 876–881. H. D. Flack, G. Bernardinelli, *J. Appl. Crystallogr.*, **2000**, *33*, 1143–1148.

Received June 3, 2002
[I02292]